

# SEMPARAMETRIC MODELING AND ANALYSIS FOR LONGITUDINAL NETWORK DATA

BY YINQIU HE<sup>1,a</sup>, JIAJIN SUN<sup>2,b</sup>, YUANG TIAN<sup>3,d</sup>,  
ZHILIANG YING<sup>2,c</sup>, AND YANG FENG<sup>4,e</sup> \*

<sup>1</sup>*Department of Statistics, University of Wisconsin-Madison, [yinqiu.he@wisc.edu](mailto:yinqiu.he@wisc.edu)*

<sup>2</sup>*Department of Statistics, Columbia University, [js5552@columbia.edu](mailto:js5552@columbia.edu); [czying@stat.columbia.edu](mailto:czying@stat.columbia.edu)*

<sup>3</sup>*Shanghai Center for Mathematical Sciences, Fudan University, [yatian20@fudan.edu.cn](mailto:yatian20@fudan.edu.cn)*

<sup>4</sup>*Department of Biostatistics, School of Global Public Health, New York University, [yang.feng@nyu.edu](mailto:yang.feng@nyu.edu)*

We introduce a semiparametric latent space model for analyzing longitudinal network data. The model consists of a static latent space component and a time-varying node-specific baseline component. We develop a semiparametric efficient score equation for the latent space parameter by adjusting for the baseline nuisance component. Estimation is accomplished through a one-step update estimator and an appropriately penalized maximum likelihood estimator. We derive oracle error bounds for the two estimators and address identifiability concerns from a quotient manifold perspective. Our approach is demonstrated using the New York Citi Bike Dataset.

**1. Introduction.** Recent years have seen increased availability of time-varying interaction/network data (Butts, 2008; Linderman and Adams, 2014; Holme, 2015), with examples such as email exchange history of coworkers (Klimt and Yang, 2004) and transport records among bike-sharing stations (CitiBike, 2019). This type of data not only includes counts of pairwise interaction events but also the timestamps of these interactions.

Non-network counting data have been studied extensively in the survival analysis literature. Andersen and Gill (1982) proposed a Poisson-type intensity-based regression model. For extensions to handle non-Poisson counting data, see Pepe and Cai (1993), Cook and Lawless (2007), Lin et al. (2000), Sun and Zhao (2013).

For cross-sectional single network data, an important development is the latent space model, in which each node is represented by a latent vector and the relationship between two nodes is quantified through their inner-product (Hoff, Raftery and Handcock, 2002). The latent vectors may be treated as random (Hoff, 2003, 2005; Bickel et al., 2013) or fixed (Athreya et al., 2018; Ma, Ma and Yuan, 2020).

Motivated by various scientific applications, multiple-network models and longitudinal network models have also been developed; see, for example, Zhang, Sun and Li (2020) for application in neuroscience, and Butts (2008) for application in social science. Similar to the single-network models, latent space modeling in the context of multiple-network settings has been examined from different perspectives (Sewell and Chen, 2015; Nielsen and Witten, 2018; Matias and Robin, 2014). One line of research views the latent vectors as random (Hoff, 2011; Salter-Townshend and McCormick, 2017), and another line considers fixed latent vectors (Jones and Rubin-Delanchy, 2020; Levin et al., 2017). The latter often leads to frequentist approaches, in which it is of common interest to study the estimation of

---

\*He, Sun, and Tian contribute equally to this work. Corresponding Author: Yang Feng.

*MSC2020 subject classifications:* Primary 62H12, 05C82; secondary 91D30, 62F12.

*Keywords and phrases:* network, counting process Poisson model, latent space model, low rank, semiparametric, heterogeneity.

shared structure across multiple networks, and in particular how the information accumulation across multiple networks improves the fitting quality (Arroyo et al., 2021; Zheng and Tang, 2022; MacDonald, Levina and Zhu, 2022; Zhang, Xue and Zhu, 2020).

In this paper, we develop a semiparametric modeling framework for longitudinal networks with interaction event counts. The model comprises a static latent space component, which accounts for inherent node interactions, and a baseline component that accommodates heterogeneity across different time points and nodes. We introduce two semiparametric estimation methods. The first method forms a generalized semiparametric one-step estimator by solving a local linear approximation of the efficient score equation. We demonstrate that the estimator automatically eliminates the identifiability issue through an interpretation in the quotient manifold induced by orthogonal transformation equivalence classes. The second method optimizes a convex surrogate loss function based on the log-likelihood, relaxing the non-convex rank constraint of the latent space component. We establish that both methods achieve, up to a logarithmic factor, the oracle estimation error rates for the latent space component.

The rest of the paper is organized as follows. Section 2 introduces the semiparametric latent space model. Section 3 introduces the one-step estimator, provides its connection to the quotient manifold theory, and establishes the error bound for the estimator. Section 4 introduces the penalized maximum likelihood estimator and establishes its error bound. Simulation results are presented in Section 5. Section 6 applies our framework to analyze the New York Citi Bike Dataset (CitiBike, 2019). Section 7 concludes the main body of the paper with some discussions. All the technical derivations are deferred to the Supplementary Material.

## 2. Semiparametric Poisson Latent Space Model.

*2.1. Notation and Model Specification.* We consider longitudinal pairwise interaction counts of  $n$  subjects (nodes) over  $T$  discrete time points. Specifically, for a time point  $t \in \{1, \dots, T\}$  and nodes  $i, j \in \{1, \dots, n\}$ ,  $A_{t,ij}$  denotes the number of  $i$ - $j$  interactions at the time point  $t$ . We propose a Poisson-based latent space model

$$(1) \quad A_{t,ij} = A_{t,ji} \sim \text{Poisson}\{\mathbb{E}(A_{t,ij} | z, \alpha)\}, \quad \text{independently with}$$

$$\mathbb{E}(A_{t,ij} | z, \alpha) = \exp(\alpha_{it} + \alpha_{jt} + \langle z_i, z_j \rangle),$$

which naturally adopts the exponential link function  $\exp(\cdot)$  to model the event counts. For any two nodes  $i$  and  $j$ , their interaction effect is modeled through the inner product of two corresponding latent vectors  $\langle z_i, z_j \rangle = z_i^\top z_j$ , similarly to the inner product model of a single network (Ma, Ma and Yuan, 2020). The latent vectors  $z_i$ 's do not change with respect to the time point  $t$  and represent the shared latent structures across  $T$  heterogeneous networks. For example,  $z_i$ 's can encode the time-invariant geographic information in multiple transportation networks. At a given time point  $t$ , when  $\alpha_{it}$  increases and all the other parameters are fixed, edges connecting the node  $i$  tend to have higher numbers of counts at the time point  $t$ , indicating higher baseline activity levels. Therefore,  $\alpha_{it}$ 's model the degree heterogeneity across different nodes  $i \in \{1, \dots, n\}$  and time points  $t \in \{1, \dots, T\}$ , and are called baseline degree heterogeneity parameters of nodes and time. In the hourly bike-sharing networks,  $\alpha_{it}$ 's can represent distinct baseline activity levels across different stations and hours.

Model specification (1) may be expressed in vector-matrix notation as

$$(2) \quad \mathbb{E}(\mathbf{A}_t | Z, \alpha) = \exp(\alpha_t \mathbf{1}_n^\top + \mathbf{1}_n \alpha_t^\top + ZZ^\top),$$

where  $\alpha_t = (\alpha_{1t}, \dots, \alpha_{nt})^\top \in \mathbb{R}^{n \times 1}$ ,  $Z = (z_1, \dots, z_n)^\top \in \mathbb{R}^{n \times k}$ ,  $\mathbf{1}_n = (1, \dots, 1)^\top \in \mathbb{R}^{n \times 1}$ , and  $\exp(\cdot)$  is the elementwise exponential operation. We consider throughout this paper the

asymptotic regime that the number of nodes  $n$  and the number of time periods  $T$  increase to infinity while the dimension of the latent space  $k$  is fixed. Thus,  $\alpha_t 1_n^\top + 1_n \alpha_t^\top + ZZ^\top$  is a low-rank matrix. To ensure identifiability, we assume that column means of  $Z$  are zero, i.e.,  $1_n^\top Z/n = 0$ . This centering assumption is analogous to the classical two-way analysis of variance (ANOVA) modeling with interaction (Scheffe, 1999). Additionally, since  $ZZ^\top = ZQQ^\top Z^\top$  for any  $Q \in \mathcal{O}(k)$ , where  $\mathcal{O}(k) = \{Q \in \mathbb{R}^{k \times k} : QQ^\top = I_k\}$ ,  $Z$  is identifiable up to a common orthogonal transformation of its rows.

Let  $\lambda_{ij,t} = \exp(\alpha_{it} + \alpha_{jt})$ . Then  $\mathbb{E}(A_{t,ij}) = \lambda_{ij,t} \times \exp(\langle z_i, z_j \rangle)$ . This form resembles the multiplicative counting process modeling in the analysis of recurrent event times (Cook and Lawless, 2007; Sun and Zhao, 2013). In particular, the  $\lambda_{ij,t}$  corresponds to the baseline rate/intensity function changing over time while the  $z_i$  corresponds to the time-invariant parameters of interest. Note that the number of baseline (nuisance) parameters is  $nT$ , and the size of the shared latent positions  $Z$  or number of parameters of interest is  $nk$ ; the former increases with both  $n$  and  $T$ , whereas the latter does not increase with  $T$ . Thus, we may be able to estimate  $Z$  more accurately than the nuisance parameter.

Some notations used in this paper are summarized as follows. For a matrix  $X = (x_{ij}) \in \mathbb{R}^{n \times n}$ ,  $\text{tr}(X) = \sum_{i=1}^n x_{ii}$  stands for its trace and  $\sigma_{\min}(X)$  represents its minimum eigenvalue. For  $X, Y \in \mathbb{R}^{n \times m}$ ,  $\langle X, Y \rangle = \text{tr}(X^\top Y)$ . If  $m \geq n$ , for any matrix  $X$  with the singular value decomposition  $X = \sum_{i=1}^n s_i u_i v_i^\top$ , we let  $\|X\|_* = \sum_{i=1}^n s_i$ ,  $\|X\|_F = \sqrt{\sum_{i=1}^n s_i^2}$ , and  $\|X\|_{\text{op}} = \max_{i=1, \dots, n} s_i$  stand for the nuclear norm, the Frobenius norm, and the operator norm of the matrix, respectively. For a vector  $x \in \mathbb{R}^n$ ,  $\|x\|_2 = \sqrt{x^\top x}$ .

For two sequences of real numbers  $\{f_n\}$  and  $\{h_n\}$ ,  $f_n \lesssim h_n$  and  $f_n = O(h_n)$  mean that  $|f_n| \leq c_1 |h_n|$  for a constant  $c_1 > 0$ ;  $f_n \asymp h_n$  means  $c_2 h_n \leq f_n \leq c_1 h_n$  for some constants  $c_1, c_2 > 0$ ;  $f_n = o(h_n)$  and  $f_n \ll h_n$  mean  $\lim_{n \rightarrow \infty} f_n/h_n = 0$ ;  $f_n \gg h_n$  means  $\lim_{n \rightarrow \infty} h_n/f_n = 0$ . For a sequence of random variables  $X_n$  and a sequence of real numbers  $f_n$ , write  $X_n = O_p(f_n)$  if for any  $\epsilon > 0$ , there exists finite  $M > 0$  such that  $\sup_n \Pr(|X_n/f_n| > M) < \epsilon$  ( $X_n/f_n$  is stochastically bounded); write  $X_n = o_p(f_n)$  if for any  $\epsilon > 0$ ,  $\lim_{n \rightarrow \infty} \Pr(|X_n/f_n| > \epsilon) = 0$  ( $X_n/f_n$  converges to 0 in probability).

**2.2. Semiparametric Oracle Error Rate and Technical Challenges.** To gain insights into the best possible error rate for estimating high-dimensional parameters, let's consider a simpler setting of the regular exponential family with a  $p_n$ -dimensional natural parameter vector  $\theta_n$ . Suppose we have  $n$  independent observations from this family. Portnoy (1988) showed that the MLE  $\hat{\theta}_n$  satisfies  $\|\hat{\theta}_n - \theta_n\|_2^2 = O_p(p_n/n)$ , where  $p_n$  can increase with the sample size  $n$ . For our problem of estimating  $Z$ , if the nuisance parameters  $\alpha$ 's were known, then each  $k$ -dimensional latent vector  $z_i$  would be measured by  $nT$  independent edges:  $\{A_{t,ij} : j = 1, \dots, n; t = 1, \dots, T\}$ . The result of Portnoy (1988) indicates that the oracle estimation error rate of each  $z_i$  would be  $k/(nT)$ . When  $k$  is fixed, the aggregated estimation error of  $n$  latent vectors  $Z = [z_1, \dots, z_n]^\top$  is expected to be of the order of  $O_p(n \times k/(nT)) = O_p(1/T)$ , which is referred to as the oracle estimation error rate throughout this paper. Since the  $\alpha$ 's are unknown, the asymptotic theory for the classical semiparametric models (Bickel et al., 1993) may be modified to yield efficient score equations (projections) so that the same error rate can be achieved.

To achieve the above oracle bounds, several technical challenges remain. Firstly, the baseline parameters  $\alpha_{it}$  in (1) not only characterize the time-specific heterogeneity over  $t$  but also represent node-specific heterogeneity over  $i$ . Due to this two-way heterogeneity, the estimation errors of  $\alpha_{it}$ 's are intertwined with those of node-specific parameters  $z_i$ 's in a complicated way. In particular, the partial likelihood (Andersen and Gill, 1982) cannot eliminate the baseline nuisance parameters. Secondly, the target parameter matrix  $Z$  is only identifiable up

to an orthogonal transformation. Therefore, given a true matrix  $Z^*$  and an estimate  $\hat{Z}$ , the ordinary Euclidean distance between the two matrices is not a proper measure for the estimation error of  $\hat{Z}$ . Indeed, it is more natural to consider their distance defined up to the orthogonal group transformation  $\text{dist}(\hat{Z}, Z^*) = \min_{Q \in \mathcal{O}(k)} \|\hat{Z} - Z^*Q\|_F$ . This distance metric indicates that the intrinsic geometry of  $Z$  is non-Euclidean. Thirdly, the estimation of  $Z$  is further challenged by the high-dimensionality of the parameters and non-linearity of the transformation in (1). Unlike classical semiparametric problems, the dimension of the parameters of interest also grows with the sample size. Furthermore, the non-linearity of the exponential link function in (1) makes it difficult for the spectral-based analyses (Arroyo et al., 2021) to deal with the entanglement between  $Z$  and  $\alpha$  and achieve the semiparametric oracle rates of  $Z$ . Lastly, the different oracle rates between different parameters also render techniques under the single network setting not easily applicable: in the single network setting  $z_i$  and  $\alpha_i$  have the same oracle rates, so it suffices to jointly control their overall error rates via the natural parameter  $\Theta_{ij} = \alpha_i + \alpha_j + \langle z_i, z_j \rangle$  from a generalized linear model perspective. In contrast, in our setting, each  $\alpha_{it}$  is measured by  $n$  independent edges:  $\{A_{t,ij} : j = 1, \dots, n\}$ , and the oracle squared error rate of each  $\alpha_{it}$  would be  $O_p(1/n)$ , compared to  $O_p(1/(nT))$  error rate of each  $z_i$ . Our goal is to attain the oracle estimation error rate of  $Z$ , which is a refinement of the overall error rate dominated by  $\alpha$ 's error.

To accurately estimate the latent space component  $Z$ , we next develop two methods: a generalized semiparametric one-step estimator in Section 3, and a semiparametric penalized maximum likelihood estimator in Section 4. We show that both methods achieve, up to a logarithmic factor, the oracle estimation error rates for the target parameters  $Z$ .

**3. Generalized Semiparametric One-Step Estimator.** In this section, we introduce our generalized semiparametric one-step estimator of  $Z$  and provide theoretical guarantees. We first introduce some notation. Model (1) leads to the following form for the log-likelihood function

$$(3) \quad L(Z, \alpha) = L(Z_v, \alpha_v) = \sum_{t=1}^T \sum_{1 \leq i \leq j \leq n} \{A_{t,ij}(\alpha_{it} + \alpha_{jt} + \langle z_i, z_j \rangle) - \exp(\alpha_{it} + \alpha_{jt} + \langle z_i, z_j \rangle)\}$$

where, for notational convenience in the differentiation of the likelihood, we use  $Z_v$  and  $\alpha_v$  to denote vectorizations of  $Z$  and  $\alpha$ , respectively, i.e.,  $Z_v = (z_1^\top, \dots, z_n^\top)^\top \in \mathbb{R}^{nk \times 1}$  and  $\alpha_v = (\alpha_1^\top, \dots, \alpha_T^\top)^\top \in \mathbb{R}^{nT \times 1}$ . Then we let  $\dot{L}_Z(Z, \alpha)$  and  $\dot{L}_\alpha(Z, \alpha)$  denote the partial derivatives of  $L(Z, \alpha)$  with respect to vectors  $Z_v$  and  $\alpha_v$ , respectively (see the precise formulae in Section C.1 of the Supplementary Material). Unless otherwise specified, such vectorization is applied when considering partial derivatives (for both first and higher orders) throughout the paper. Following the semiparametric literature (Tsiatis, 2006), the efficient score and the efficient Fisher information matrix for  $Z$  can be expressed as

$$(4) \quad \begin{aligned} S_{eff}(Z, \alpha) &= \dot{L}_Z - \mathbb{E}(\dot{L}_Z \dot{L}_\alpha^\top) \{ \mathbb{E}(\dot{L}_\alpha \dot{L}_\alpha^\top) \}^{-1} \dot{L}_\alpha \in \mathbb{R}^{nk \times 1}, \\ I_{eff}(Z, \alpha) &= \mathbb{E}(S_{eff}(Z, \alpha) S_{eff}^\top(Z, \alpha)) \in \mathbb{R}^{nk \times nk}, \end{aligned}$$

where, for notational simplicity,  $(Z, \alpha)$  is omitted in  $\dot{L}_Z$  and  $\dot{L}_\alpha$ .

With the above preparations, we construct our generalized semiparametric one-step estimator as

$$(5) \quad \hat{Z}_v = \check{Z}_v + \{I_{eff}(\check{Z}, \check{\alpha})\}^+ S_{eff}(\check{Z}, \check{\alpha}),$$

where  $(\check{Z}, \check{\alpha})$  denotes an initial estimate, and  $B^+$  represents the Moore–Penrose inverse of a matrix  $B$ , which is uniquely defined and also named pseudo inverse (Ben-Israel and Greville, 2003). By the property of pseudo inverse, (5) can be equivalently written as

$$(6) \quad \hat{Z}_v = \check{Z}_v + \check{U} \left\{ \check{U}^\top I_{eff}(\check{Z}, \check{\alpha}) \check{U} \right\}^{-1} \check{U}^\top S_{eff}(\check{Z}, \check{\alpha}),$$

where  $\check{U}$  is a matrix whose columns can be any set of basis of the column space of  $I_{eff}(\check{Z}, \check{\alpha})$ .

The estimator originates from the one-step estimator for semiparametric problems (Van der Vaart, 2000, Section 25.8), which solves the efficient score equation in the presence of nuisance parameters through a linear approximation at an initial estimate. However, different from the classical one-step estimator, the efficient information matrix is singular in our setting; see Remark 1. As a result, the corresponding linear approximation equations are under-determined. Taking pseudo inverse corresponds to solving the linear approximation equation with minimum  $\ell_2$  norm; the solution lies in the column space of  $\check{U}$ , as indicated in (6).

Owing to the intricate technical challenges outlined in Section 2.2 and the singularity of  $I_{eff}(\check{Z}, \check{\alpha})$ , straightforward conclusions regarding the classical one-step estimator for (5) are elusive. However, we have constructed a detailed semiparametric analysis and demonstrated that our proposed one-step estimator nearly achieves the oracle error rate, given suitable initial estimators. We will present the comprehensive theoretical results in the following Section 3.1. Additionally, in Section 3.4, we will introduce an initial estimator that demonstrates both statistical suitability and computational efficiency.

**REMARK 1.** *In effect, the singularity of the efficient information matrix  $I_{eff}(Z, \alpha)$  is caused by the redundancy and unidentifiability of parameters in  $Z$  (Little, Heidenreich and Li, 2010). Particularly, we find that the rank of  $I_{eff}(Z, \alpha)$  equals  $nk - k(k+1)/2$ , which is identical to the number of free parameters in the  $n \times k$  matrix  $Z$ . Below we provide a high-level explanation, and please find a formal justification in Lemma 6 in Section A.1. Firstly, recall that to avoid the mean shift issue in (2), we have imposed  $k$  linear constraints  $\mathbf{1}_n^\top Z = 0$ . Secondly, even with the centering constraints,  $Z$  can only be identified up to an orthogonal group transformation  $\mathcal{O}(k)$ . In particular,  $\mathcal{O}(k)$  is the orthogonal Stiefel manifold, and its dimension is  $k(k-1)/2$  (see, e.g., Absil, Mahony and Sepulchre, 2009, Section 3.3.2). Intuitively,  $k + k(k-1)/2 = k(k+1)/2$  degrees of freedom are removed due to the constraints and unidentifiability. This leads to  $nk - k(k+1)/2$  number of free parameters in  $Z$ .*

**3.1. Theory.** Throughout the sequel, we use  $(Z^*, \alpha^*)$  to denote the true value of  $(Z, \alpha)$ . In other words, our observed data follow the model (1) with  $(Z, \alpha) = (Z^*, \alpha^*)$ . Besides, we denote  $\Theta_{t,ij} = \alpha_{it} + \alpha_{jt} + \langle z_i, z_j \rangle$ . We define the estimation error from the  $i$ -th row of  $\check{Z}$  as  $\text{dist}_i(\check{z}_i, z_i^*) = \|\check{z}_i - \check{Q}^\top z_i^*\|_2$ , where

$$(7) \quad \check{Q} = \arg \min_{Q \in \mathcal{O}(k)} \|\check{Z} - Z^*Q\|_F,$$

so that  $\text{dist}^2(\check{Z}, Z^*) = \sum_{i=1}^n \text{dist}_i^2(\check{z}_i, z_i^*)$ . The goal in this subsection is to establish error bound for the proposed one-step estimator (5) in terms of the distance defined above. To do so we need the following regularity conditions.

**CONDITION 1.** *Assume the true parameters  $\alpha^*$ 's and  $z^*$ 's satisfy:*

- (i) *There exist positive constants  $M_{Z,1}$ ,  $M_\alpha$ , and  $M_{\Theta,1}$  such that  $\|z_i^*\|_2^2 \leq M_{Z,1}$ ,  $|\alpha_{it}^*| \leq M_\alpha$ , and  $\Theta_{t,ij}^* \leq -M_{\Theta,1}$  for  $1 \leq i, j \leq n$  and  $1 \leq t \leq T$ ;*
- (ii) *There exists a positive constant  $M_{Z,2}$  such that  $\sigma_{\min}[(Z^*)^\top Z^*/n] \geq M_{Z,2}$ ;*
- (iii)  $\mathbf{1}_n^\top Z^* = 0$ .

CONDITION 2. Assume the initial estimates  $\check{\alpha}$ 's and  $\check{z}$ 's satisfy :

- (i) There exist constants  $M_b > 0$  and  $\epsilon$  such that  $|\check{\alpha}_{it} - \alpha_{it}^*| + \text{dist}_i(\check{z}_i, z_i^*) \leq M_b n^{-1/2} \log^\epsilon(nT)$  for  $1 \leq i \leq n$  and  $1 \leq t \leq T$ ;
- (ii)  $\mathbf{1}_n^\top \check{Z} = 0$ .

Condition 1(i) assumes boundedness of the true parameters. It also implies  $-M_{\Theta,2} \leq \Theta_{t,ij}^* \leq -M_{\Theta,1}$  with  $M_{\Theta,2} = M_{Z,1} + 2M_\alpha$ . Condition 1(ii) excludes degenerate cases of  $Z^*$ . This, together with  $\|z_i^*\|_2^2 \leq M_{Z,1}$ , indicates  $\|Z^*\|_{\text{op}} \asymp \sqrt{n}$ . Condition 1(iii) is needed in order to identify the interaction effects  $Z^*(Z^*)^\top$  in (2). Condition 2(ii) requires  $\check{Z}$  to be a feasible estimator satisfying the centering constraint. With this condition,  $\hat{Z}$  is guaranteed to be feasible, namely  $\mathbf{1}_n^\top \hat{Z} = 0$ . Condition 2(i) is analogous to the “ $\sqrt{n}$ -consistent initial estimator” used in the classical one-step estimator (Van der Vaart, 2000). It assumes that the estimation errors of  $\check{\alpha}_{it}$ 's and  $\check{z}_i$ 's are uniformly bounded by  $M_b \log^\epsilon(nT)/\sqrt{n}$ . In Section 3.4, we will construct an initial estimator satisfying Condition 2 with the error bound of order  $\log^2(nT)/\sqrt{n}$  under high probability. Recall that the classical MLE theory indicates that the optimal estimation errors for individual  $\alpha_{it}$  and  $z_i$  would be of the orders of  $n^{-1/2}$  and  $(nT)^{-1/2}$ , respectively. In this regard, the constructed initial  $\check{\alpha}_{it}$  achieves its optimal rate up to a logarithmic factor. On the other hand, Condition 2(i) assumes that  $\check{z}_i$  achieves the same error rate as  $\check{\alpha}_{it}$  but not its own optimal rate  $(nT)^{-1/2}$ . In this connection, Condition 2 imposes a mild assumption on the initial  $\check{z}_i$ 's. We also would like to point out that the deterministic upper bounds in Condition 2(i) may be relaxed to probabilistic upper bounds. The current non-probabilistic bounds are used to simplify the presentation. Theorem 1 below establishes the near optimality of the proposed one-step estimator (5).

THEOREM 1. Assume Conditions 1–2. Let  $\hat{Z}$  be the generalized one-step estimator defined as in (5). Let  $\varsigma = \max\{\epsilon, 1/2\}$ . For any constant  $s > 0$ , there exists a constant  $C_s > 0$  such that when  $n/\log^{2\varsigma}(T)$  is sufficiently large,

$$\Pr \left\{ \text{dist}^2(\hat{Z}, Z^*) > \frac{1}{T} \times C_s r_{n,T} \right\} = O(n^{-s}),$$

where  $r_{n,T} = \max \left\{ 1, \frac{T}{n} \right\} \log^{4\varsigma}(nT)$ .

Theorem 1 implies that with high probability, the estimation error  $\text{dist}^2(\hat{Z}, Z^*)$  is  $O(r_{n,T}/T)$ . For ease of understanding, we first ignore the logarithmic term in  $r_{n,T}$ , i.e., set  $\varsigma = 0$ . Then the error order reduces to

$$(8) \quad \frac{1}{T} \times \max \left\{ 1, \frac{T}{n} \right\} = \max \left\{ \frac{1}{T}, \frac{1}{n} \right\}.$$

When  $T = 1$ , i.e., for a single network, (8) =  $O(1)$  achieves the oracle error rate. This is similar to Ma, Ma and Yuan (2020), which studied a single network; also see Section 3.2 for a detailed discussion. When  $1 < T \lesssim n$ , (8) =  $O(1/T)$ , indicating that our proposed generalized one-step estimator achieves the oracle estimation error rate in this case. When  $T \gg n$ , (8) =  $O(1/n)$ , which unfortunately, is not exactly inverse proportional to  $T$ . Intuitively, when  $T$  is very large, there is too much time heterogeneity, resulting in too many nuisance parameters  $\alpha_{it}$ 's over time and in turn, causing the technical difficulty of analyzing the target  $Z$ . Nevertheless, we still have (8) =  $O(1/n)$ , which is smaller than the optimal error rate  $O(1)$  for a single network. This suggests that given  $T > 1$  networks, the estimation error of  $Z$  can always be improved compared to using only a single network. This can be interpreted, in a broad sense, as an “inverse proportional to  $T$ ” property. We call  $O(1/n)$  a sub-oracle rate throughout the paper.

Compared to (8), the established error bound  $r_{n,T}/T$  contains an extra logarithmic term  $\log^{4\varsigma}(nT)$ , which comes from the uniform error control over high-dimensional parameters  $(\alpha, Z)$  and the initialization error in Condition 2(i). As an example, we propose an initial estimator in Section 3.4 satisfying  $\varsigma = \epsilon = 2$ . For a finite  $\varsigma$ , the error bound  $O(r_{n,T}/T)$ , similarly to (8), decreases as  $T$  increases. To sum up, up to logarithmic factors,  $\hat{Z}$  achieves the oracle error rate  $O(1/T)$ , when  $1 \leq T \lesssim n$ , and  $\hat{Z}$  achieves the sub-oracle error rate  $O(1/n)$ , when  $T \gg n$ .

REMARK 2. *The efficient Fisher information matrix  $I_{eff}$  in (6) can also be replaced by the “observed efficient information matrix” defined as  $-H_{eff}$ , where*

$$H_{eff}(Z, \alpha) = \ddot{L}_{Z,Z}(Z, \alpha) - \ddot{L}_{Z,\alpha}(Z, \alpha) \ddot{L}_{\alpha,\alpha}^{-1}(Z, \alpha) \ddot{L}_{\alpha,Z}(Z, \alpha)$$

satisfies  $\mathbb{E}\{-H_{eff}(Z, \alpha)\} = I_{eff}(Z, \alpha)$ . In that case, the one-step estimator is given by

$$(9) \quad \check{Z}_v - \check{U} \left\{ \check{U}^\top H_{eff}(\check{Z}, \check{\alpha}) \check{U} \right\}^{-1} \check{U}^\top S_{eff}(\check{Z}, \check{\alpha}),$$

and theoretically, we could establish the same rate as that in Theorem 1. More details on this are provided in Section D.2 of the Supplementary Material.

REMARK 3. *To establish the near-oracle rate in Theorem 1, the key idea is to show that through our semiparametric efficient construction, the estimation error of  $\alpha_{it}$ 's would not mask that of  $z_i$ 's. Intuitively, this is achievable due to the fact  $\mathbb{E}\left\{\frac{\partial S_{eff}(Z, \alpha)}{\partial \alpha_{it}}\right\} = 0$ . This shows that a small perturbation error of  $\alpha_{it}$ 's would not change the efficient score of  $z_i$ 's in terms of the first-order expansion and therefore, its influence on estimating  $z_i$ 's can be reduced (Bickel et al., 1993). Nevertheless, establishing the near-oracle rate of  $Z$  is still challenged by the complex structures of  $\alpha$  and  $Z$  under our model (1).*

For the nuisance parameters  $\alpha$ , we do not impose any structural assumptions, such as smoothness or sparsity. Therefore,  $\alpha_{it}$ 's can be completely heterogeneous over all  $i \in \{1, \dots, n\}$  and  $t \in \{1, \dots, T\}$ , and the free dimension of  $\alpha$  is  $nT$ . Such two-way heterogeneity and high dimensionality of  $\alpha$  make it difficult to separate the estimation error of  $\alpha$  from that of  $Z$  as discussed in Section 2.2. Technically, we reduce the influence of estimating  $\alpha$  by carefully investigating the semiparametric efficient score. But that influence cannot be eliminated entirely, which causes a sub-oracle rate when  $T$  is very large, as shown in (8).

For the target parameters  $Z$ , the non-Euclidean geometry and identifiability constraints of  $Z$  lead to the singularity of the efficient information matrix  $I_{eff}(\check{Z}, \check{\alpha})$  as mentioned in Remark 1. To address the issue, we explicitly characterize a restricted subspace of  $\mathbb{R}^{nk}$  on which  $I_{eff}(\check{Z}, \check{\alpha})$  has positive eigenvalues. The restricted eigenspace exhibits interesting properties for characterizing the estimation error of  $\hat{Z}$  and has fundamental connections with two sources of identifiability constraints of  $Z$  in Remark 1. Please see details in Section A.1.

3.2. *Related Works.* Various models have been proposed for multiple heterogeneous networks. We briefly review related works focusing on fixed-effect continuous latent vectors.

One class of multiple-network models generalizes the random dot product graphs (Athreya et al., 2018; Rubin-Delanchy et al., 2022). For example, Arroyo et al. (2021) considered settings with  $T$  layers of networks, and in the  $t$ -th layer network with  $1 \leq t \leq T$ , each edge  $A_{t,ij} = A_{t,ji} \sim \text{Bernoulli}\{\mathbb{E}(A_{t,ij})\}$  independently for  $1 \leq t \leq T$  and  $1 \leq i < j \leq n$ , where  $\mathbb{E}(A_{t,ij}) = \langle z_i, z_j \rangle_{\Lambda_t}$  with  $\langle z_i, z_j \rangle_{\Lambda_t} = z_i^\top \Lambda_t z_j$ . Here  $z_i$ 's denote the common latent positions shared across  $T$  networks, and  $\Lambda_t \in \mathbb{R}^{k \times k}$  characterizes the layer-specific latent information. A similar model for directed random graphs has been studied in Zheng and Tang (2022) with non-symmetric latent positions shared across  $T$  networks. MacDonald, Levina and Zhu

(2022) proposed models based on generalized random dot product graphs and established theoretical results when  $A_{t,ij} \sim \text{Normal}\{\mathbb{E}(A_{t,ij}), \sigma^2\}$  independently, where  $\sigma$  is a nuisance parameter, and  $\mathbb{E}(A_{t,ij}) = \langle z_i, z_j \rangle_{I_{p_1, q_1}} + \langle u_{i,t}, u_{j,t} \rangle_{I_{p_2, t, q_2, t}}$ . Here  $z_i$ 's denote the shared latent vectors, whereas  $u_{i,t}$ 's denote the layer-specific latent vectors, and  $\langle \cdot, \cdot \rangle_{I_{p,q}}$  defines an indefinite inner product, where  $I_{p,q} = \text{diag}(1, \dots, 1, -1, \dots, -1)$  with  $p$  ones followed by  $q$  negative ones on its diagonal for  $p \geq 1$  and  $q \geq 0$ .

From the perspective of generalized linear models, the above models can be viewed as linear responses with the identity link function. Considering a single network with binary edges, Hoff, Raftery and Handcock (2002) proposed models with the logit link function, and Ma, Ma and Yuan (2020) proposed and analyzed two estimation methods. Generalizing the idea to multilayer binary networks, Zhang, Xue and Zhu (2020) proposed the following model: for  $t = 1, \dots, T$  layers of networks, each edge  $A_{t,ij} \sim \text{Bernoulli}\{\mathbb{E}(A_{t,ij})\}$  independently for  $1 \leq i, j \leq n$ , where  $\mathbb{E}(A_{t,ij}) = \text{logit}^{-1}(\alpha_{it} + \alpha_{jt} + \langle z_i, z_j \rangle_{\Lambda_t})$  with  $\text{logit}^{-1}(x) = e^x / (1 + e^x)$ .

Under the above models, one common interest is to estimate the latent vectors  $Z = [z_1, \dots, z_n]^\top$  shared across multiple heterogeneous networks. Table 1 summarizes the squared estimation error rates for  $Z$  in four studies with a focus on the order of the error with respect to  $n$  and  $T$  only. Our results and intuition on the oracle error rate are consistent with some existing results. But establishing similar results under our model (1) requires non-trivial technical developments due to various challenges including two-way heterogeneity, high-dimensionality, and non-linearity of the link function as discussed in Section 2.2. To the best of our knowledge, for multiple networks ( $T > 1$ ) with *non-linear* link functions in models, there is no existing result that is comparable to our derived nearly optimal rate in Theorem 1.

TABLE 1  
Squared Estimation Error Rates of Shared Latent Vectors  $z_i$ 's in Different Models.

	Models with Identity Link		Models with Logit Link	
Model	Arroyo et al. (2021)	MacDonald et al. (2022)	Ma et al. (2020) ( $T = 1$ )	Zhang et al. (2020)
Error Order	$O\left(\frac{1}{T} + \frac{1}{n}\right)$	$O\left(\frac{n^\eta}{T}\right)$ ( $\eta \geq 0$ )	$O(1)$	$O\left(1 + \frac{1}{T}\right)$

3.3. *Geometric Interpretation on Quotient Manifold.* The proposed (6) treats the  $n \times k$  matrix  $Z$  as an  $nk$ -dimensional vector  $Z_v$ . This ignores the constraint of the space  $\mathbb{R}_0^{n \times k} = \{Z \in \mathbb{R}^{n \times k} : \mathbf{1}_n^\top Z = 0, \det(Z^\top Z) \neq 0\}$ . Moreover, viewing  $Z$  as an element of  $\mathbb{R}_0^{n \times k}$  ignores that it is identified up to a rotation under our considered log-likelihood  $L(Z, \alpha)$ , as  $L(Z, \alpha) = L(ZQ, \alpha)$  for any  $Q \in \mathcal{O}(k)$ . Interestingly, in our considered problem, we find that (6) implicitly takes the underlying parameter structure into account.

To demonstrate this, we first show the intrinsic parameter space of  $Z$  is a quotient set. In particular, the ‘‘rotation invariance’’ naturally induces an equivalence relation on  $\mathbb{R}_0^{n \times k}$ :  $Z_1 \sim Z_2$  if and only if there exists  $Q \in \mathcal{O}(k)$  such that  $Z_2 = Z_1 Q$ . Given the equivalence relation  $\sim$  on  $\mathbb{R}_0^{n \times k}$  and an element  $Z \in \mathbb{R}_0^{n \times k}$ , elements in  $\mathbb{R}_0^{n \times k}$  that are equivalent to  $Z$  form an equivalence class of  $Z$ , denoted as  $[Z]$ . The set of equivalence classes of all elements in  $\mathbb{R}_0^{n \times k}$  is called the quotient set, denoted as  $\mathbb{R}_0^{n \times k} / \sim$ . Equipped with the equivalence relation  $\sim$ , the quotient set  $\mathbb{R}_0^{n \times k} / \sim$  naturally incorporates the rotation invariance of  $Z$  and thus is the intrinsic parameter space to examine. For the simplicity of notation, we let  $\mathcal{M}$  denote  $\mathbb{R}_0^{n \times k} / \sim$  below.



We next show that (6) can be viewed as an approximation to the one-step Newton-Raphson update of the log profile likelihood on the quotient set  $\mathcal{M}$ . Specifically, the log profile likelihood of  $Z$  is  $pL(Z) = L(Z, \hat{\alpha}(Z))$  with  $\hat{\alpha}(Z) = \arg \max_{\alpha \in \mathbb{R}^{n \times \tau}} L(Z, \alpha)$ . The MLE of  $Z$ , i.e., the first component of  $(\hat{Z}_{\text{MLE}}, \hat{\alpha}_{\text{MLE}})$  that maximizes  $L(Z, \alpha)$ , is also the maximizer of  $pL(Z)$ . Therefore, to investigate the MLE of the target parameter  $Z$ , it suffices to examine  $pL(Z)$  (Murphy and Van der Vaart, 2000). On the quotient set  $\mathcal{M}$ ,  $pL(Z)$  naturally induces a function  $pL_Q : \mathcal{M} \rightarrow \mathbb{R}$  with  $pL_Q([Z]) = pL(Z)$  for any  $Z \in \mathbb{R}_0^{n \times k}$ . To incorporate the rotation invariance relation, it is natural to search for the maximizer of  $pL_Q$  on the quotient set  $\mathcal{M}$ . Fortunately, a Newton-Raphson step for  $pL_Q$  can be properly constructed given the nice properties of  $\mathcal{M}$  and  $pL_Q$  in Lemma 2.

LEMMA 2 (Lee, 2013, Chapter 21). *On  $\mathbb{R}_0^{n \times k}$ , consider the canonical atlas  $\varphi : \mathbb{R}_0^{n \times k} \rightarrow \mathbb{R}^{(n-1)k}$  given by  $\varphi(Z) = (z_1^\top, \dots, z_{n-1}^\top)^\top$ , and the canonical Riemannian metric  $g_Z(Z_1, Z_2) = \text{tr}(Z_1^\top Z_2)$  for  $Z_1$  and  $Z_2$  in the tangent space to  $\mathbb{R}_0^{n \times k}$  at  $Z$ . (i) Endowed with the differential structure and the Riemannian metric induced by that of  $\mathbb{R}_0^{n \times k}$ , the quotient set  $\mathcal{M}$  is a smooth Riemannian quotient manifold of dimension  $nk - k(k+1)/2$ . (ii)  $pL_Q : \mathcal{M} \rightarrow \mathbb{R}$  is a smooth function.*

In particular, consider the Riemannian manifold  $\mathcal{M}$  equipped with the Riemannian connection and the exponential retraction  $R$  (Absil, Mahony and Sepulchre, 2009, Section 5). For a smooth function  $f : \mathcal{M} \rightarrow \mathbb{R}$ , the Newton-Raphson update at an equivalence class  $[Z] \in \mathcal{M}$  is given by  $R_{[Z]}(\nu)$ , where  $\nu$  is a tangent vector in the tangent space  $T_{[Z]}\mathcal{M}$  and specified by  $\text{Hess } f([Z])[\nu] = -\text{Grad } f([Z])$ , and  $\text{Hess } f([Z])$  and  $\text{Grad } f([Z])$  denote the Hessian and gradient of  $f$  at  $[Z]$ , respectively (Boumal, 2023). Conceptually,  $R_{[Z]}(\nu)$  defines a move in the direction of  $\nu$  while staying on the manifold. Interestingly, for the function  $pL_Q$ , we prove that  $R_{[Z]}(\nu)$  has an analytic (matrix) form in Proposition 3.

PROPOSITION 3. *Under the same setting as Lemma 2, equip  $\mathcal{M}$  with the Riemannian connection and the exponential retraction  $R$ . Consider an initial value  $\check{Z}$  and its equivalence class  $[\check{Z}]$ . For  $pL_Q$  at  $[\check{Z}]$ , the Newton-Raphson update  $R_{[\check{Z}]}(\nu) = [\text{mat}(\check{Z}_v + \bar{\nu}_{\check{Z}})]$ , where  $\check{Z}_v$  is the vectorization of  $\check{Z}$ ,  $\text{mat}((z_1^\top, \dots, z_n^\top)^\top) = (z_1, \dots, z_n)^\top \in \mathbb{R}^{n \times k}$ , and*

$$\bar{\nu}_{\check{Z}} = -\check{U} \left[ \check{U}^\top H_{eff} \{ \check{Z}, \hat{\alpha}(\check{Z}) \} \check{U} \right]^{-1} \check{U}^\top S_{eff} \{ \check{Z}, \hat{\alpha}(\check{Z}) \},$$

where  $\check{U}$  is the same as that in (6), and  $H_{eff}(Z, \alpha)$  is defined same as in Remark 2.

We can see that  $\check{Z}_v + \bar{\nu}_{\check{Z}}$  is similar to (9) except that  $\hat{\alpha}(\check{Z})$  is replaced with  $\check{\alpha}$ . Given initial values  $(\check{Z}, \check{\alpha})$  that are close to the true values  $(Z^*, \alpha^*)$ , our theoretical analysis indicates that  $\hat{\alpha}(\check{Z})$  and  $\check{\alpha}$  are close, and thus  $\check{Z}_v + \bar{\nu}_{\check{Z}}$  and (9) are close. By Remark 2, (5), (6), and (9) can all be viewed as approximations to a one-step Newton-Raphson update on the quotient manifold  $\mathcal{M}$ , whose construction implicitly incorporates the underlying geometric structures of the quotient manifold.

REMARK 4. *We provide an intuitive explanation of Proposition 3. Motivated by the fact that the log profile likelihood  $pL(Z)$  depends on parameters in  $Z$  only through  $ZZ^\top$ , we next focus on  $ZZ^\top$ . For ease of visualization, we first consider the parameter space  $\mathbb{S}_0^{2 \times 2} = \{Z \in \mathbb{R}^{2 \times 2} : \frac{1}{2} Z^\top Z = 0_{1 \times 2}\}$ . For  $Z \in \mathbb{S}_0^{2 \times 2}$ ,  $ZZ^\top = (z_{11}^2 + z_{12}^2)(1, -1)^\top(1, -1)$  depends on  $Z$  only through the scalar  $z_{11}^2 + z_{12}^2$ . This suggests that the number of free parameters in  $ZZ^\top$  is 1, which equals  $nk - k(k+1)/2$  as analyzed in Remark 1. We visualize the function*

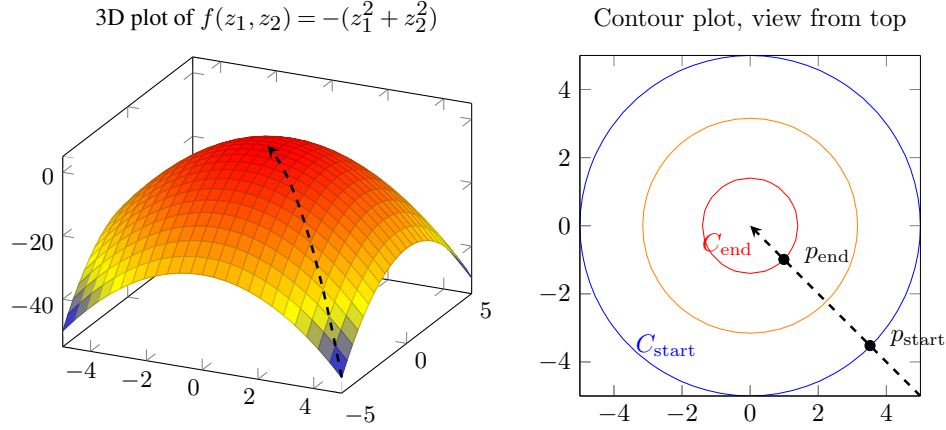


Fig 1: Each circle represents one equivalence class of  $(z_1, z_2)$  giving the same value of  $\bar{f}(z_1, z_2)$ . It suffices to search for maximization along one given direction.

$\bar{f}(z_{11}, z_{12}) = -(z_{11}^2 + z_{12}^2)$  in Figure 1. The function has a constant value on each circle of  $(z_{11}, z_{12})$  in the contour plot. From this perspective, each circle is an equivalence class giving the same value of  $\bar{f}$ . The set of all equivalence classes (circles) yields a quotient set, denoted as  $\mathcal{M}_2$ , and  $\bar{f}$  induces a function  $f: \mathcal{M}_2 \rightarrow \mathbb{R}$  given by  $f([z]) = \bar{f}(z_{11}, z_{12})$ , where  $[z] \in \mathcal{M}_2$  represents the equivalence class specified by  $(z_{11}, z_{12})$ .

Consider the problem of maximizing the function  $f$  on  $\mathcal{M}_2$ . One natural idea is to search for the maximizer of  $f$  across its domain  $\mathcal{M}_2$ . In this case, an update step in  $\mathcal{M}_2$  yields a move from one circle to another, e.g.,  $C_{start}$  to  $C_{end}$  in Figure 1. Such an abstract update can also be described in the Euclidean space  $\mathbb{R}^2$ . In particular, fix one direction that is orthogonal to a tangent line of circles, e.g., the dashed line in Figure 1, move along the tangent line from the point  $p_{start}$  to the point  $p_{end}$  in Figure 1, and map  $p_{end}$  to the corresponding equivalence class  $C_{end}$ . The update from  $p_{start}$  to  $p_{end}$  in  $\mathbb{R}^2$  can be analytically represented in a matrix form. Generalizing this idea, an update step on the quotient manifold  $\mathbb{R}_0^{n \times k} / \sim$  can be described through a fixed search space in the Euclidean space  $\mathbb{R}^{n \times k}$  (analogous to the search direction in Figure 1), and a common choice is the so-called horizontal space (Boumal, 2023). Interestingly, we prove that the horizontal space at  $\check{Z}$  can be explicitly expressed through  $\check{U}$ . This enables us to derive an analytic form  $\bar{v}_{\check{Z}}$ , which, after properly aligned into a matrix, defines an update in the horizontal space. The retraction  $R$  maps the post-update matrix  $\text{mat}(\check{Z}_v + \bar{v}_{\check{Z}})$  to an element in  $\mathbb{R}_0^{n \times k} / \sim$ , which gives the targeted one-step estimator in the manifold.

**3.4. Initial Estimation.** In this section, we construct an initial estimator  $(\check{Z}, \check{\alpha})$  and prove that it satisfies Condition 2 with  $\epsilon = 2$  and high probability. The proposed initialization algorithm consists of two stages outlined below, while the implementation details are provided in Section E.1 of the Supplementary Material. In the following, we define  $E_t^* = \mathbb{E}(\mathbf{A}_t)$ ,  $\Theta_t^* = \log(E_t^*)$  for  $t = 1, \dots, T$ , and  $G^* = Z^*(Z^*)^\top$ . We note that

$$(10) \quad \alpha_t^* = H_n^{-1} \Theta_t^* \mathbf{1}_n, \quad \text{and} \quad G^* = \sum_{t=1}^T (\Theta_t^* - \alpha_t^* \mathbf{1}_n^\top - \mathbf{1}_n (\alpha_t^*)^\top) / T,$$

where  $H_n = n\mathbf{I}_n + \mathbf{1}_n \mathbf{1}_n^\top$ .

*Outline of the Initialization Algorithm.*

- (1) The first stage obtains an “initial of initial” estimator  $(\check{Z}, \check{\alpha})$  as follows. A similar “double-SVD” idea has been introduced in [Zhang, Chen and Li \(2020\)](#).
  - (a) Construct an estimator  $\check{E}_t$  for  $E_t^*$  by applying the universal singular value thresholding ([Chatterjee, 2015](#)) to each matrix  $\mathbf{A}_t$ . Take  $\check{\Theta}_t = \log(\check{E}_t)$  as an estimator for  $\Theta_t^*$ .
  - (b) Let  $\check{\alpha}_t = H_n^{-1} \check{\Theta}_t \mathbf{1}_n$ , motivated by (10). Take  $\check{\alpha} = (\check{\alpha}_1, \dots, \check{\alpha}_T)$ .
  - (c) Let  $\check{G} = \sum_{t=1}^T (\check{\Theta}_t - \check{\alpha}_t \mathbf{1}_n^\top - \mathbf{1}_n \check{\alpha}_t^\top) / T$ , motivated by (10).  
Let  $\check{Z} = \check{U}_k \check{D}_k^{1/2}$ , where  $\check{U}_k \check{D}_k \check{U}_k^\top$  denote the top- $k$  eigen-decomposition of  $\check{G}$ .
- (2) The second stage utilizes the projected gradient descent method ([Chen and Wainwright, 2015](#)) with  $L(Z, \alpha)$  as an objective function to maximize, and  $(\check{Z}, \check{\alpha})$  from the first stage as initial values. In particular,
  - (a) Update  $Z$  and  $\alpha$  along their corresponding gradient directions with pre-specified step sizes.
  - (b) Project the updated estimates to the constraint set  $\mathcal{S}_C$  induced by the conditions of identifiability and boundedness of parameters in Condition 1. Specifically,
 
$$\mathcal{S}_C = \{(Z, \alpha) : Z \in \mathbb{R}^{n \times k}, \mathbf{1}_n^\top Z = 0, \max_i \|z_i\|_2^2 \leq M_{Z,1}, \alpha \in \mathbb{R}^{n \times T}, \max_{i,t} |\alpha_{it}| \leq M_\alpha\}.$$
  - (c) Repeat (a) and (b) until convergence. The resulting values, denoted as  $(\check{Z}, \check{\alpha})$ , are used as the initial estimator in the proposed one-step estimator.

In Theorem 4, we establish an elementwise error bound of  $(\check{Z}, \check{\alpha})$  obtained through the proposed initialization algorithm above.

**THEOREM 4.** *Assume Condition 1. For any constant  $s > 0$ , there exists a constant  $C_s > 0$  such that when  $n / \log^{k+3}(T)$  is sufficiently large,*

$$\Pr \left[ \max_{1 \leq i \leq n, 1 \leq t \leq T} \{|\check{\alpha}_{it} - \alpha_{it}^*| + \text{dist}_i(\check{z}_i, z_i^*)\} > \frac{C_s \log^2(nT)}{\sqrt{n}} \right] = O((nT)^{-s}).$$

Theorem 4 implies that with high probability, the initial estimator  $(\check{Z}, \check{\alpha})$  satisfy Condition 2 with  $\epsilon = 2$ .

**4. Semiparametric Penalized Maximum Likelihood Estimator.** The log-likelihood  $L(Z, \alpha)$  is non-convex in  $Z$ , and also requires specification of the dimension of each  $z_i$ . On the other hand, when the log-likelihood (3) is reparametrized through  $G = (G_{ij})_{n \times n}$  with  $G_{ij} = \langle z_i, z_j \rangle$ , the log-likelihood function

$$l(G, \alpha) = \sum_{t=1}^T \sum_{1 \leq i \leq j \leq n} [A_{t,ij}(\alpha_{it} + \alpha_{jt} + G_{ij}) - \exp(\alpha_{it} + \alpha_{jt} + G_{ij})]$$

is convex in  $\alpha$  and  $G$ . Nevertheless,  $G = ZZ^\top$  itself overparameterizes the model, and the dimension of  $z_i$  corresponds to the rank of  $G$  in this model specification. Subject to the rank constraint, solving MLE of  $G$  is a non-convex optimization problem, even though  $l(G, \alpha)$  is convex. To overcome this issue, we construct a penalized maximum likelihood estimator of  $G$  with a nuclear norm penalization that relaxes the exact rank constraint on  $G$ . We further show that the proposed estimator can achieve the corresponding almost-oracle error rate.

We first characterize the parameter space of  $G$  and its relationship with  $Z$ . From the perspective of likelihood functions, matrices  $G$  and  $Z$  such that  $L(Z, \alpha) = l(G, \alpha)$  can be viewed

as equivalent parameters. Accordingly, any  $Z \in \mathbb{R}_0^{n \times k}$  uniquely defines  $G = ZZ^\top \in \mathbb{S}_{0,+}^{n,k}$ , where  $\mathbb{S}_{0,+}^{n,k}$  represents the class of all  $n \times n$  positive semidefinite symmetric matrices with rank  $k$  and  $G1_n = 0_n$ . Moreover, any matrix  $G \in \mathbb{S}_{0,+}^{n,k}$  induces  $G^{1/2} = U_k D_k^{1/2} \in \mathbb{R}_0^{n \times k}$ , where  $U_k D_k U_k^\top$  is the top- $k$  eigenvalue components of  $G$ . Then  $G$  uniquely identifies an equivalence class  $\{G^{1/2}Q : Q \in \mathcal{O}(k)\} = \{Z \in \mathbb{R}_0^{n \times k} : ZZ^\top = G\}$ .

The penalized maximum likelihood estimator is defined as the solution  $(\hat{G}, \hat{\alpha})$  to the following convex optimization problem

$$(11) \quad \max_{G, \alpha} \quad l(G, \alpha) - \lambda_{n,T} \|G\|_*$$

$$\text{subject to } G \in \mathbb{S}_+^n, \quad G1_n = 0_n, \quad |G_{ij}| \leq M_{Z,1},$$

where  $\mathbb{S}_+^n$  represents the class of  $n \times n$  positive semidefinite matrices,  $M_{Z,1}$  is a constant same as in Condition 1, and  $\lambda_{n,T}$  is a prespecified tuning parameter.

To scale the error of  $G$  to the error of  $Z$ , we present the estimation error of  $G$  in terms of  $\|\hat{G} - G^*\|_{\mathbb{F}}^2/n$ ; see Remark 5. The following Theorem 5 shows that the penalized MLE  $\hat{G}$  solved from (11) almost achieves the oracle rate, similarly to Theorem 1.

**THEOREM 5.** *Assume  $G^* = Z^* Z^{*\top}$  with  $Z^* \in \mathbb{R}_0^{n \times k}$  satisfying Condition 1. Suppose we choose  $\lambda_{n,T} \asymp \sqrt{nT} \log(nT)$ . Then for any constant  $s > 0$ , there exists a constant  $C_s > 0$  such that when  $n/\log(T)$  is sufficiently large,*

$$\Pr \left\{ \|\hat{G} - G^*\|_{\mathbb{F}}^2/n > \frac{1}{T} \times C_s r'_{n,T} \right\} = O(n^{-s}),$$

where  $r'_{n,T} = \max \left\{ 1, \frac{T}{n} \right\} \log^2(nT)$ .

Theorem 5 implies that with high probability, the estimation error  $\|\hat{G} - G^*\|_{\mathbb{F}}^2/n$  is  $O(r'_{n,T}/T)$ . Similarly to Theorem 1, when ignoring the logarithmic term in  $r'_{n,T}/T$ , the error order reduces to (8). Therefore, up to the logarithmic term, the penalized MLE achieves the oracle estimation error rate  $O(1/T)$  when  $1 \leq T \lesssim n$ , and it achieves the sub-oracle rate  $O(1/n)$  when  $T \gg n$ .

**REMARK 5.** *Intuitively,  $n^2$  parameters in  $G^*$  are redundant and essentially determined by only  $nk$  parameters in  $Z^*$ . To align with the error rate in Theorem 1, we consider the estimation error of  $\hat{G}$  with a scaling factor  $1/n$  in Theorem 5. When the rank  $k$  is known, the one-step estimator  $\hat{Z}$  induces the estimator  $\hat{Z}\hat{Z}^\top$  for  $G^*$  satisfying  $\|\hat{Z}\hat{Z}^\top - G^*\|_{\mathbb{F}}^2/n \asymp \text{dist}^2(\hat{Z}, Z^*) \asymp 1/T$ ; see Lemmas H.3 and H.4 in the Supplementary Material. When  $k$  is unknown, Theorem 5 suggests the penalized MLE  $\hat{G}$  achieves the same error rate as that of  $\hat{Z}\hat{Z}^\top$ .*

**REMARK 6.** *Given  $\hat{G}$  solved from (11), we can further construct an estimator for  $Z^*$ . If the true  $k$  is given, we let  $\hat{Z}_k = \hat{U}_k \hat{D}_k^{1/2}$ , where  $\hat{U}_k \hat{D}_k \hat{U}_k^\top$  is the top- $k$  eigenvalue components of the penalized MLE  $\hat{G}$ . When  $k$  is unknown, it can be consistently estimated from the eigenvalues of  $\hat{G}$ . We draw a general conclusion that given any estimator  $\hat{G}_0 \in \mathbb{R}^{n \times n}$  satisfying  $\|\hat{G}_0 - G^*\|_{\mathbb{F}}^2/n = o_p(n^{1-2\epsilon})$  for a fixed constant  $\epsilon \in (0, 1/2)$ ,  $k$  can be consistently estimated as the number of eigenvalues of  $\hat{G}_0$  that are greater than  $n^{1-\epsilon}$ .*

**REMARK 7.** *The idea of using the nuclear norm penalization as a convex relaxation of the exact rank constraint originates from the low-rank matrix recovery literature (Candès*

and Tao, 2010; Candès and Recht, 2012; Davenport et al., 2014). It was also utilized by Ma, Ma and Yuan (2020) to fit the latent space model for a single network. But different from these studies, we have two components  $G$  and  $\alpha$  in our model with different but entangling oracle error rates. To establish a sharp error rate for  $\hat{G}$ , we develop a novel semiparametric analysis for the penalized MLE through the profile likelihood (Murphy and Van der Vaart, 2000).

In particular, we note that  $\hat{G}$  is also the penalized MLE of the log profile likelihood  $pl(G) = l(G, \hat{\alpha}(G))$ , where  $\hat{\alpha}(G) = \arg \max_{\alpha \in \mathbb{R}^{n \times \tau}} l(G, \alpha)$ . Let  $\dot{l}_\alpha$  and  $\ddot{l}_{\alpha\alpha}$  represent the first-order derivatives and the second-order derivatives of  $l(G, \alpha)$  with respect to  $\alpha_v$ , respectively. We can obtain  $\hat{\alpha}(G) - \alpha = (\ddot{l}_{\alpha\alpha})^{-1} \dot{l}_\alpha + \text{high-order terms}$ , and  $\mathbb{E}(\dot{l}_\alpha) = 0$ . Intuitively, this suggests that the perturbation error from  $\hat{\alpha}(G)$  can be small in terms of the first-order expansions, so its impact on the profile likelihood of  $G$  can be reduced.

Despite the wide use of the profile likelihood method (Murphy and Van der Vaart, 2000; Severini and Wong, 1992), our analysis is faced with unique technical challenges. First, not only are the nuisance parameters  $\alpha$  high-dimensional but also they encode two-way heterogeneity over both nodes and time. As a result, to separate the estimation error of  $G$  from that of  $\alpha$  requires delicate analysis that differs significantly from the existing studies. Second, the target parameter  $G$  is high-dimensional and intrinsically redundant with a low-rank structure. The redundancy of parameters in  $G$ , as explained in Remark 1, leads to singularity issues when analyzing the likelihood function and calls for new technical developments. Meanwhile, the low-rank structure of  $G$  motivates the use of the nuclear norm penalization, which needs to be properly taken care of in our semiparametric analysis.

**REMARK 8 (Relationship between the two estimators).** Both estimators are motivated by maximizing the semiparametric profile likelihood. In particular, the penalized MLE is a convex relaxation of maximizing the log-likelihood function  $l(ZZ^\top, \alpha)$ , which is equivalent to maximizing the log profile likelihood  $pL(Z)$ . The one-step estimator solves the maximization of the quadratic function  $q(x) = pL(\check{Z}) + (x - \check{Z}_v)^\top S_{eff}(\check{Z}, \check{\alpha}) - \frac{1}{2}(x - \check{Z}_v)^\top I_{eff}(\check{Z}, \check{\alpha})(x - \check{Z}_v)$ . In settings with fixed-dimensional target parameters, the log profile likelihood is approximated by its local quadratic expansion similar to  $q(x)$  (Murphy and Van der Vaart, 2000). From an alternative point of view, the one-step estimator gives an approximate solution to the efficient score equation, which in general is equivalent to maximizing the profile likelihood. Therefore, we expect that the two proposed estimators are similar up to the convex relaxation, and they can achieve the oracle error rate as the nuisance  $\alpha$  is eliminated through the profile likelihood.

**5. Simulation Studies.** We conduct simulation studies to examine how the estimation errors vary with respect to  $n$  and  $T$ . To this end, we consider the following two scenarios of  $(n, T)$ :

- (a) fixing  $n = 200$  and varying  $T \in \{5, 10, 20, 40, 80\}$ ;
- (b) fixing  $T = 20$  and varying  $n \in \{100, 200, 400, 800\}$ .

In each scenario, we allow varying  $k \in \{2, 4, 8\}$ . Given  $(n, T, k)$ , we generate the shared latent vectors  $Z^*$  as follows: independently sample  $w_i$  following a uniform distribution on  $\mathbb{B}_2^k = \{x \in \mathbb{R}^k : \|x\|_2 \leq 1\}$ , let  $W = [\tilde{w}_1, \dots, \tilde{w}_n]^\top$  where  $\tilde{w}_j = w_j - \sum_{l=1}^n w_l/n$ , and set  $Z^* = \sqrt{n}W/\|WW^\top\|_F^{1/2}$ . In this way,  $Z^*$  has zero column means, and  $G^* = Z^*Z^{*\top}$  satisfies  $\|G^*\|_F/n = 1$ . For the baseline heterogeneity parameters  $\alpha^*$ , we consider two cases

- (I)  $\alpha_{it}^*$  are independently sampled from  $U(-2, 0)$ ;
- (II)  $\alpha_{it}^* = t/T + \beta_{it}$  with  $\beta_{it}$  independently sampled from  $U(-3, -1)$  for  $1 \leq i \leq \lfloor n/2 \rfloor$ , and  $\alpha_{it}^* = -2t/T + \beta_{it}$  with  $\beta_{it}$  independently sampled from  $U(-2, 0)$  for  $\lfloor n/2 \rfloor < i \leq n$ .

Intuitively,  $\alpha^*$ 's in Cases (I) and (II) represent different types of heterogeneity; the former is uniform over  $i$ , whereas the latter has a two-block structure over  $i$ .

Under each model configuration and for each estimator, we estimate the error  $\text{dist}^2(\hat{Z}, Z^*)$  over 50 Monte Carlo simulations. We compute  $\text{dist}^2(\hat{Z}, Z^*) = \|\hat{Z} - Z^* V U^\top\|_F^2$  where  $U \Sigma V^\top$  is the singular value decomposition of  $\hat{Z}^\top Z^*$ ; see Schönemann (1966). For the penalized MLE, we obtain  $\hat{Z}$  following Remark 6 given true  $k$ ; the corresponding errors of  $\hat{G}$  follow similar patterns and are provided in Section I.1 of the Supplementary Material.

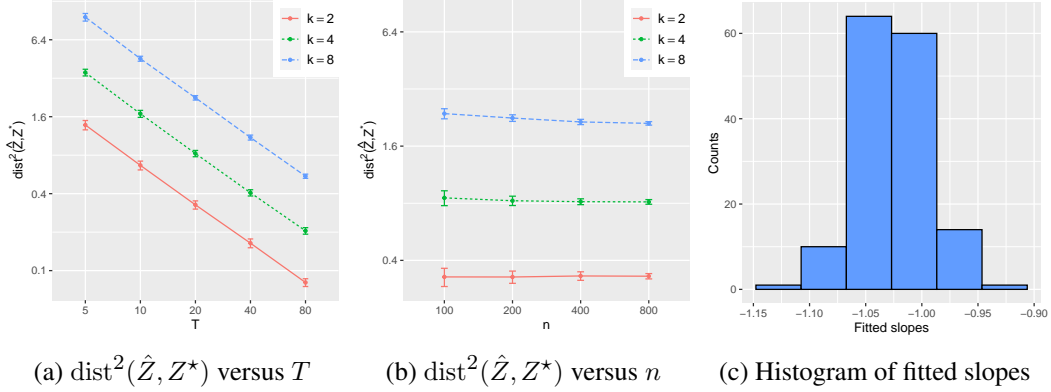


Fig 2: Case (I): Empirical estimation errors of the one-step estimator. Panel (a) presents  $\text{dist}^2(\hat{Z}, Z^*)$  (averaged over 50 repetitions) versus  $T$  in the scenario (a). Panel (b) presents  $\text{dist}^2(\hat{Z}, Z^*)$  (averaged over 50 repetitions) versus  $n$  in the scenario (b). In (a) and (b), axes are in the log scale, three lines correspond to results under  $k \in \{2, 4, 8\}$ , respectively, and error bars are obtained by  $\pm$  the standard deviation from 50 repetitions. Panel (c) presents the slopes from regressing  $\log \text{dist}^2(\hat{Z}, Z^*)$  on  $\log T$  with fixed  $(n, k) \in \{200\} \times \{2, 4, 8\}$  in the 50 repetitions under the scenario (a).

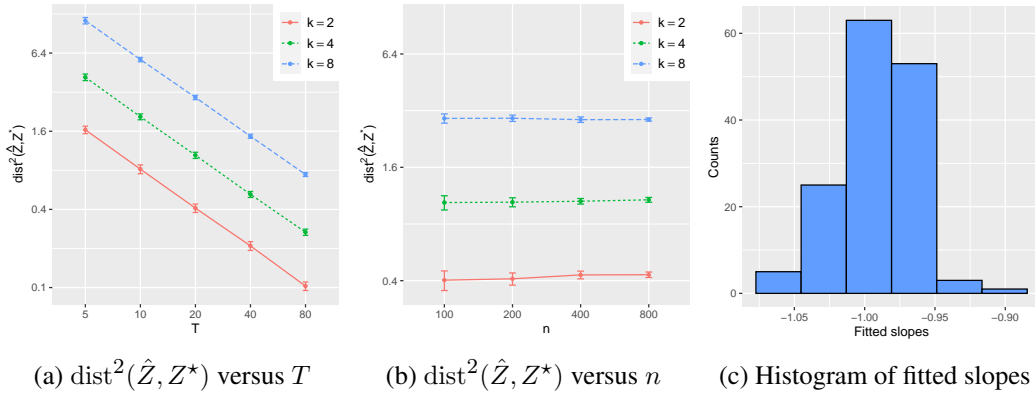


Fig 3: Case (I): Empirical estimation errors of the penalized MLE. Panels (a)–(c) are presented similarly to Figure 2.

Under Case (I), we present the empirical estimation errors of the one-step estimator and the penalized MLE in Figures 2 and 3, respectively. In each figure, panel (a) suggests that

$\text{dist}^2(\hat{Z}, Z^*)$  is inverse proportional to  $T$  when  $n$  is fixed. Furthermore, panel (c) shows that all the fitted slopes are close to  $-1$ . In addition, panel (b) shows that  $\text{dist}^2(\hat{Z}, Z^*)$  does not change too much as  $n$  increases. In conclusion, the numerical results are consistent with the oracle theoretical rate  $O(1/T)$  for the estimation error of  $Z^*$ . Comparing Figures 2 and 3, we find that under the same  $(n, T, k)$ , the one-step estimator can achieve a slightly smaller estimation error than the penalized MLE. This might be because biases are introduced with the convex relaxation. But the penalized MLE could be more flexible and robust when the true  $k$  is unknown in applications. Under Case (II), we present the empirical estimation errors  $\text{dist}^2(\hat{Z}, Z^*)$  of the one-step estimator and the penalized MLE in Figures 4 and 5, respectively. We can see that the patterns are similar to those in Figures 2–3. The results suggest the oracle theoretical rate  $O(1/T)$  can hold under a variety of types of heterogeneity of  $\alpha^*$ .

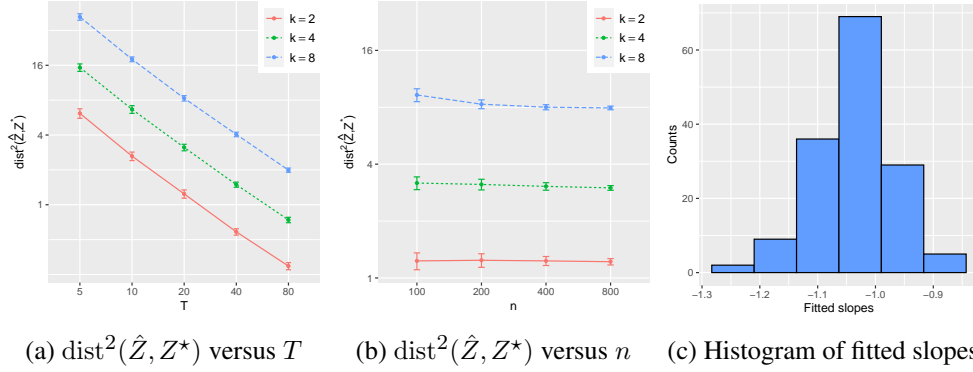


Fig 4: Case (II): Empirical estimation errors of the one-step estimator. Panels (a)–(c) are presented similarly to Figure 2.

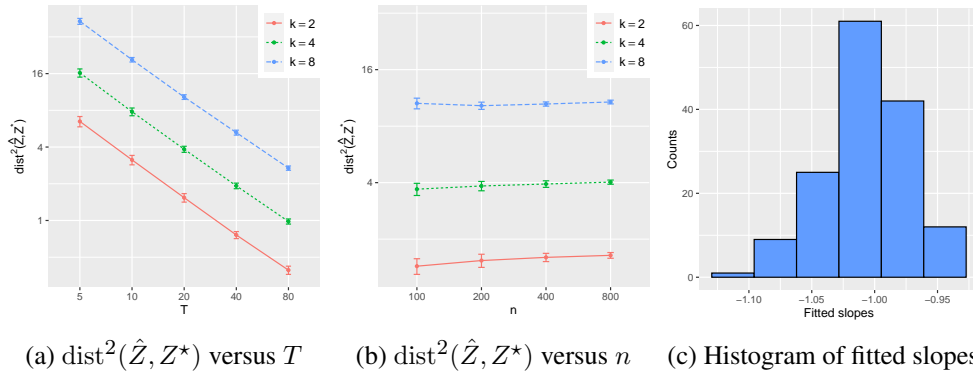


Fig 5: Case (II): Empirical estimation errors of the penalized MLE. Panels (a)–(c) are presented similarly to Figure 2.

**6. Analysis of New York Citi Bike Dataset.** We illustrate the use of the proposed methods by analyzing the New York Citi Bike data (CitiBike, 2019). The data set contains over 2.3 million rides between bike stations in New York in August 2019. Each ride is identified by two stations and a time stamp (the hire starting time). We focus on a weekday, August

1st, 2019 and keep the rides that last between one minute and 3 hours. The processed data contains 85,854 rides between 782 stations over 24 hours. The 782 bike stations form a common set of nodes across hours. A pair of stations defines a network edge, and the number of events between them in each hour gives the hourly edge weight. We provide exploratory data visualization in Figure 6. Panels (b) and (c) of Figure 6 show that the number of ride events is very heterogeneous across different bike stations and hours, respectively, motivating the application of the model (1).

We next fit the model (1) with 2-dimensional latent vectors  $z_i$ 's. The choice of  $k = 2$  is for the ease of interpretation below and is consistent with the strategy in Remark 6. Figure 7 (a) visualizes the estimated positions  $\hat{z}_i$ 's obtained by the one-step estimator, while the results of the penalized MLE are similar and deferred to the Supplementary Material.

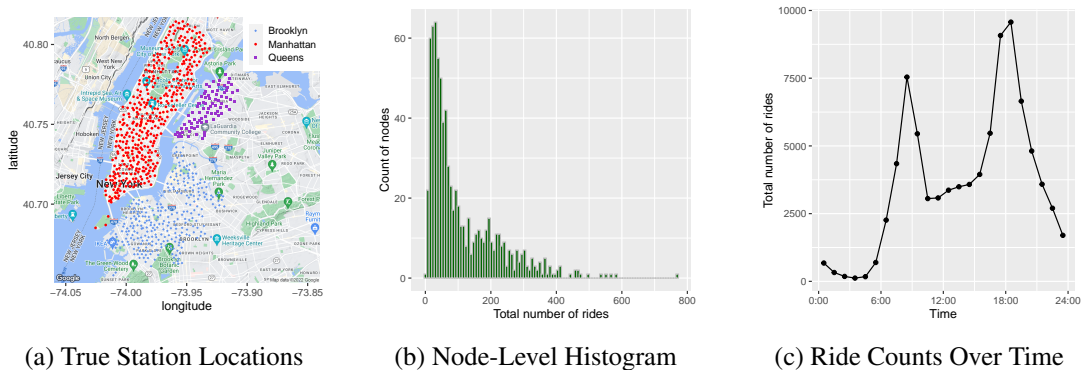


Fig 6: Illustration of Citi Bike Data: Panel (a) presents true locations of bike stations on Google Map, colored by three boroughs of New York City. Panel (b) presents the histogram of the total number of rides by nodes (bike stations). Panel (c) presents the total number of rides over the 24-hour period.

To interpret the results, we compare the estimated latent space vectors  $\hat{z}_i$ 's, visualized in Figure 7 (a), with true geographic locations (in latitudes and longitudes) of stations, visualized in Figure 6 (a). We can see that overall, the estimated latent positions can match the true geographic positions. Particularly, the stations located in Manhattan are well-separated from those in Brooklyn and Queens. This could be because the borough Manhattan is separated from the other two boroughs by the East River, and it is less common to use shared bikes to travel between Manhattan and the other two boroughs. On the other hand, the estimated station locations in Brooklyn and Queens overlap. This could be because Queens and Brooklyn are not physically divided by a river, and it is easier to travel between these two boroughs by biking. In the meantime, some bike stations were estimated to be in the Central Park area. This could be because people would ride through Central Park frequently, so two stations that are far away geographically might be viewed as close to each other based on the interactions. Besides the latent vectors, we visualize the estimated baseline levels across the 24-hour period in Figure 7 (c). The results show a time-varying pattern that is consistent with the true changing pattern of the total number of rides across the 24-hour periods, visualized in Figure 6 (c). In summary, the fitted parameters  $\hat{z}_i$ 's and  $\hat{\alpha}_{it}$ 's under the model (1) are reasonable and interpretable.

In addition, comparing panels (a) and (b) in Figure 7, we can see that the alignment between the estimated latent space vectors and the true geographic locations improves as we utilize observations over more hours. The results suggest that the proposed methods can



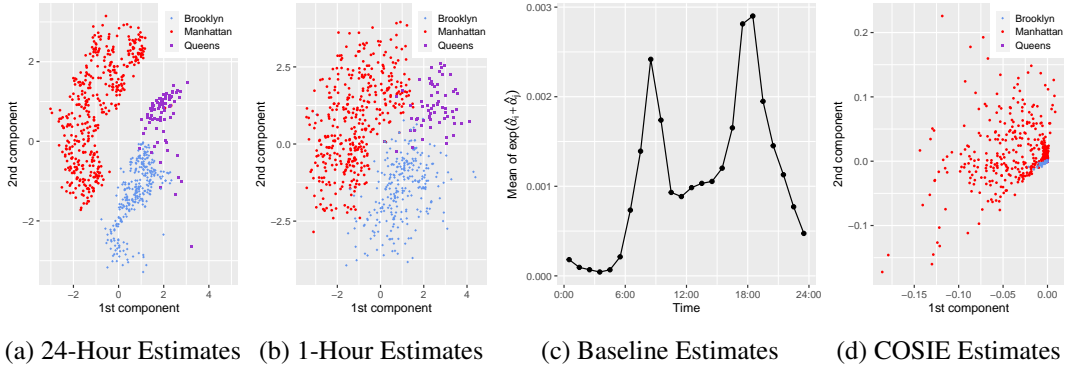


Fig 7: Estimation Results: Panel (a) shows the estimated latent positions  $\hat{z}_i \in \mathbb{R}^2$  using all the data across the 24-hour period. Each point is colored based on which borough the corresponding bike station is located, and we present the results after a rotation for better visualization. Panel (b) shows the estimated latent positions  $\hat{z}_i \in \mathbb{R}^2$  using one-hour data during 21:00-22:00 on the selected day, where points are similarly colored and rotated to those in the panel (a). Panel (c) presents the mean of estimated baseline levels  $\sum_{i,j=1}^n \exp(\hat{\alpha}_{it} + \hat{\alpha}_{jt})/n^2$  for  $t = 1, \dots, 24$ , i.e., across the 24-hour period under the model (1). Panel (d) presents the estimated two-dimensional shared latent vectors under COSIE with 24-hour data.

effectively extract static latent space information and accommodate time heterogeneity simultaneously.

As a comparison, we fit the data by the common subspace independent edge (COSIE) model in Arroyo et al. (2021) with two-dimensional shared latent vectors. We estimate the model by the multiple adjacency spectral embedding (MASE) method in Arroyo et al. (2021). We present the estimated latent vectors in Figure 7 (d). Compared to Figure 7 (a), Figure 7 (d) does not appear to show a direct connection between the estimated latent positions and the geographic positions of bike stations. This may be because Arroyo et al. (2021) targeted at  $\mathbf{A}_t$ 's that are adjacency matrices with binary edges. We present the results by COSIE only to illustrate the differences between different mean models of  $\mathbf{A}_t$ 's.

**7. Discussion.** In this work, we propose a longitudinal latent space model tailored for recurrent interaction events. We develop two novel semiparametric estimation techniques, i.e., the generalized semiparametric one-step updating and the penalized maximum likelihood estimation, and show that the resulting estimators attain the oracle estimation error rate for the shared latent structure. The first approach utilizes the semiparametric efficient score equation to construct a second-order updating estimator. We show that the estimator possesses a geometric interpretation on the quotient manifold, which automatically overcomes the non-uniqueness issue due to overparametrization. The second approach corresponds to a convex relaxation of the low-rank static latent space component.

By separating the (primary) parameters of interest associated with the static latent space from the dynamic nuisance parameters, a strategy commonly found in semiparametrically efficient parameter estimation, we are able to delineate the oracle rates of convergence for the primary and the nuisance parameters according to their dimensions. This strategy also helps us to untangle the static and time-heterogeneous components inherent in the network model and construct the oracle estimators.

There are a few other interesting future works. First, the ability to accurately estimate latent structures could enable important downstream analysis such as prediction, hypothesis testing, and change-point detection. For instance, it may be useful to ascertain a change point

in the structure of the latent space (Bhattacharjee, Banerjee and Michailidis, 2020; Enikeeva and Klopp, 2021; Padilla, Yu and Priebe, 2022). The achievement of oracle estimation error rates could facilitate the quantification of uncertainty in estimators, which in turn lays a strong foundation for conducting reliable statistical inference.

Second, this paper focuses on the variance in estimation error rates as a function of  $n$  and  $T$ , while treating the latent dimension  $k$  and network sparsity level as fixed. Extending the current methodology and theory to the cases when  $k$  grows (Choi, Wolfe and Airoldi, 2012) as well as sparse networks (Qin and Rohe, 2013; Le, Levina and Vershynin, 2017) are important topics.

Finally, it would be worthwhile to generalize our results to other models, including directed networks, various distributions for weighted edges, continuous time stamps, or additional covariates influencing the network structure (Hoff, Raftery and Handcock, 2002; Vu et al., 2011; Perry and Wolfe, 2013; Hoff, 2015; Kim et al., 2018; Sit, Ying and Yu, 2021; Weng and Feng, 2021; Huang, Sun and Feng, 2023). We believe that the proposed semiparametric analysis framework can function as a valuable building block for establishing sharp estimation error rates under those models.

**Acknowledgments.** Ying was partially supported by NSF Grant DMS-2015417. Feng was partially supported by NIH grant 1R21AG074205-01, NYU University Research Challenge Fund, and a grant from NYU School of Global Public Health.

## SUPPLEMENTARY MATERIAL

### Supplement to “Semiparametric Modeling and Analysis for Longitudinal Network Data.”

Due to space limitation, additional results and proofs are deferred to the supplementary material.

## REFERENCES

- ABSIL, P.-A., MAHONY, R. and SEPULCHRE, R. (2009). *Optimization algorithms on matrix manifolds*. Princeton University Press.
- ANDERSEN, P. K. and GILL, R. D. (1982). Cox’s regression model for counting processes: a large sample study. *The Annals of Statistics* **10** 1100–1120.
- ARROYO, J., ATHREYA, A., CAPE, J., CHEN, G., PRIEBE, C. E. and VOGELSTEIN, J. T. (2021). Inference for multiple heterogeneous networks with a common invariant subspace. *Journal of Machine Learning Research* **22** 1–49.
- ATHREYA, A., FISHKIND, D. E., TANG, M., PRIEBE, C. E., PARK, Y., VOGELSTEIN, J. T., LEVIN, K., LYZINSKI, V., QIN, Y. and SUSSMAN, D. L. (2018). Statistical Inference on Random Dot Product Graphs: a Survey. *Journal of Machine Learning Research* **18** 1–92.
- BEN-ISRAEL, A. and GREVILLE, T. N. (2003). *Generalized inverses: theory and applications* **15**. Springer Science & Business Media.
- BHATTACHARJEE, M., BANERJEE, M. and MICHAILIDIS, G. (2020). Change point estimation in a dynamic stochastic block model. *Journal of Machine Learning Research* **21** 4330–4388.
- BICKEL, P. J., KLAASSEN, C. A., BICKEL, P. J., RITOV, Y., KLAASSEN, J., WELLNER, J. A. and RITOV, Y. (1993). *Efficient and adaptive estimation for semiparametric models*. Springer.
- BICKEL, P., CHOI, D., CHANG, X. and ZHANG, H. (2013). Asymptotic normality of maximum likelihood and its variational approximation for stochastic blockmodels. *The Annals of Statistics* **41** 1922–1943.
- BOUMAL, N. (2023). *An introduction to optimization on smooth manifolds*. Cambridge University Press.
- BUTTS, C. T. (2008). A relational event framework for social action. *Sociological Methodology* **38** 155–200.
- CANDÈS, E. J. and RECHT, B. (2012). Exact matrix completion via convex optimization. *Communications of the ACM* **55** 111–119.
- CANDÈS, E. J. and TAO, T. (2010). The power of convex relaxation: Near-optimal matrix completion. *IEEE Transactions on Information Theory* **56** 2053–2080.

- CHATTERJEE, S. (2015). Matrix estimation by universal singular value thresholding. *The Annals of Statistics* **43** 177–214.
- CHEN, S., LIU, S. and MA, Z. (2022). Global and individualized community detection in inhomogeneous multilayer networks. *The Annals of Statistics* **50** 2664–2693.
- CHEN, Y. and WAINWRIGHT, M. J. (2015). Fast low-rank estimation by projected gradient descent: General statistical and algorithmic guarantees. *arXiv preprint arXiv:1509.03025*.
- CHOI, D. S., WOLFE, P. J. and AIROLDI, E. M. (2012). Stochastic blockmodels with a growing number of classes. *Biometrika* **99** 273–284.
- CITIBIKE (2019). New York Citi Bike Data in August 2019. <https://github.com/cedoula/bikesharing>. [Original source: <https://ride.citibikenyc.com/system-data>].
- COOK, R. J. and LAWLESS, J. F. (2007). *The statistical analysis of recurrent events*. Springer.
- DAVENPORT, M. A., PLAN, Y., VAN DEN BERG, E. and WOOTTERS, M. (2014). 1-bit matrix completion. *Information and Inference: A Journal of the IMA* **3** 189–223.
- ENIKEEVA, F. and KLOPP, O. (2021). Change-point detection in dynamic networks with missing links. *arXiv preprint arXiv:2106.14470*.
- HOFF, P. D. (2003). *Random effects models for network data*. Citeseer.
- HOFF, P. D. (2005). Bilinear mixed-effects models for dyadic data. *Journal of the American Statistical Association* **100** 286–295.
- HOFF, P. D. (2011). Hierarchical multilinear models for multiway data. *Computational Statistics & Data Analysis* **55** 530–543.
- HOFF, P. D. (2015). Multilinear tensor regression for longitudinal relational data. *The annals of applied statistics* **9** 1169–1193.
- HOFF, P. D., RAFTERY, A. E. and HANDCOCK, M. S. (2002). Latent space approaches to social network analysis. *Journal of the American Statistical Association* **97** 1090–1098.
- HOLME, P. (2015). Modern temporal network theory: a colloquium. *The European Physical Journal B* **88** 1–30.
- HUANG, S., SUN, J. and FENG, Y. (2023). PCABM: Pairwise Covariates-Adjusted Block Model for Community Detection. *Journal of the American Statistical Association*.
- JONES, A. and RUBIN-DELANCHY, P. (2020). The multilayer random dot product graph. *arXiv preprint arXiv:2007.10455*.
- KIM, B., NIU, X., HUNTER, D. R. and CAO, X. (2018). A dynamic additive and multiplicative effects model with application to the United Nations voting behaviors. *arXiv preprint arXiv:1803.06711*.
- KLIMT, B. and YANG, Y. (2004). The enron corpus: A new dataset for email classification research. In *European conference on machine learning* 217–226. Springer.
- LE, C. M., LEVINA, E. and VERSHYNIN, R. (2017). Concentration and regularization of random graphs. *Random Structures & Algorithms* **51** 538–561.
- LEE, J. M. (2013). *Introduction to smooth manifolds*. Springer.
- LEVIN, K., ATHREYA, A., TANG, M., LYZINSKI, V. and PRIEBE, C. E. (2017). A central limit theorem for an omnibus embedding of multiple random dot product graphs. In *2017 IEEE international conference on data mining workshops (icdmw)* 964–967. IEEE.
- LIN, D. Y., WEI, L.-J., YANG, I. and YING, Z. (2000). Semiparametric regression for the mean and rate functions of recurrent events. *Journal of the Royal Statistical Society: Series B (Statistical Methodology)* **62** 711–730.
- LINDERMAN, S. and ADAMS, R. (2014). Discovering latent network structure in point process data. In *International conference on machine learning* 1413–1421.
- LITTLE, M. P., HEIDENREICH, W. F. and LI, G. (2010). Parameter identifiability and redundancy: theoretical considerations. *PLoS ONE* **5** e8915.
- MA, Z., MA, Z. and YUAN, H. (2020). Universal Latent Space Model Fitting for Large Networks with Edge Covariates. *Journal of Machine Learning Research* **21** 1–67.
- MACDONALD, P. W., LEVINA, E. and ZHU, J. (2022). Latent space models for multiplex networks with shared structure. *Biometrika* **109** 683–706.
- MATIAS, C. and MIELE, V. (2017). Statistical clustering of temporal networks through a dynamic stochastic block model. *Journal of the Royal Statistical Society: Series B (Statistical Methodology)* **79** 1119–1141.
- MATIAS, C., REBAFKA, T. and VILLERS, F. (2018). A semiparametric extension of the stochastic block model for longitudinal networks. *Biometrika* **105** 665–680.
- MATIAS, C. and ROBIN, S. (2014). Modeling heterogeneity in random graphs through latent space models: a selective review. *ESAIM: Proceedings and Surveys* **47** 55–74.
- MURPHY, S. A. and VAN DER VAART, A. W. (2000). On profile likelihood. *Journal of the American Statistical Association* **95** 449–465.
- NIELSEN, A. M. and WITTEN, D. (2018). The multiple random dot product graph model. *arXiv preprint arXiv:1811.12172*.

- PADILLA, O. H. M., YU, Y. and PRIEBE, C. E. (2022). Change point localization in dependent dynamic non-parametric random dot product graphs. *Journal of Machine Learning Research* **23** 10661–10719.
- PEPE, M. S. and CAI, J. (1993). Some graphical displays and marginal regression analyses for recurrent failure times and time dependent covariates. *Journal of the American Statistical Association* **88** 811–820.
- PERRY, P. O. and WOLFE, P. J. (2013). Point process modelling for directed interaction networks. *Journal of the Royal Statistical Society: Series B (Statistical Methodology)* **75** 821–849.
- PORTNOY, S. (1988). Asymptotic behavior of likelihood methods for exponential families when the number of parameters tends to infinity. *The Annals of Statistics* **16** 356–366.
- QIN, T. and ROHE, K. (2013). Regularized spectral clustering under the degree-corrected stochastic blockmodel. *Advances in neural information processing systems* **26**.
- RUBIN-DELANCHY, P., CAPE, J., TANG, M. and PRIEBE, C. E. (2022). A statistical interpretation of spectral embedding: The generalised random dot product graph. *Journal of the Royal Statistical Society: Series B (Statistical Methodology)* **84** 1446–1473.
- SALTER-TOWNSHEND, M. and MCCORMICK, T. H. (2017). Latent space models for multiview network data. *The annals of applied statistics* **11** 1217–1244.
- SCHEFFE, H. (1999). *The analysis of variance* **72**. John Wiley & Sons.
- SCHÖNEMANN, P. H. (1966). A generalized solution of the orthogonal procrustes problem. *Psychometrika* **31** 1–10.
- SEVERINI, T. A. and WONG, W. H. (1992). Profile likelihood and conditionally parametric models. *The Annals of Statistics* **20** 1768–1802.
- SEWELL, D. K. and CHEN, Y. (2015). Latent space models for dynamic networks. *Journal of the American Statistical Association* **110** 1646–1657.
- SIT, T., YING, Z. and YU, Y. (2021). Event history analysis of dynamic communication networks. *Biometrika* **108** 223–230.
- SUN, J. and ZHAO, X. (2013). *Statistical analysis of panel count data*. Springer.
- TSIATIS, A. A. (2006). *Semiparametric theory and missing data*. Springer.
- VAN DER VAART, A. W. (2000). *Asymptotic statistics* **3**. Cambridge university press.
- VU, D., HUNTER, D., SMYTH, P. and ASUNCION, A. (2011). Continuous-time regression models for longitudinal networks. In *Advances in Neural Information Processing Systems* 2492–2500.
- WENG, H. and FENG, Y. (2021). Community detection with nodal information: likelihood and its variational approximation. *Stat* e428.
- XU, K. S. and HERO, A. O. (2014). Dynamic stochastic blockmodels for time-evolving social networks. *IEEE Journal of Selected Topics in Signal Processing* **8** 552–562.
- YANG, T., CHI, Y., ZHU, S., GONG, Y. and JIN, R. (2011). Detecting communities and their evolutions in dynamic social networks—a Bayesian approach. *Machine learning* **82** 157–189.
- ZHANG, J. and CHEN, Y. (2020). Modularity based community detection in heterogeneous networks. *Statistica Sinica* **30** 601–629.
- ZHANG, H., CHEN, Y. and LI, X. (2020). A note on exploratory item factor analysis by singular value decomposition. *Psychometrika* **85** 358–372.
- ZHANG, J., SUN, W. W. and LI, L. (2020). Mixed-effect time-varying network model and application in brain connectivity analysis. *Journal of the American Statistical Association* **115** 2022–2036.
- ZHANG, X., XUE, S. and ZHU, J. (2020). A flexible latent space model for multilayer networks. In *International Conference on Machine Learning* 11288–11297.
- ZHENG, R. and TANG, M. (2022). Limit results for distributed estimation of invariant subspaces in multiple networks inference and PCA. *arXiv preprint arXiv:2206.04306*.